Supplementary data

Revealing the contributions of DFT to the spectral interpretation for amino benzoyl thiourea derivative: Insights into experimental studies from theoretical perspectives, and biological evaluation

Ahmed M. Hegazy [a], Nesreen S. Haiba [b], Mohamed K. Awad [c], Mohamed Teleb[d], and Faten M. Atlam [c]*

[a] Department of Materials Science, Institute of Graduate Studies and Research, Alexandria University, Egypt.

[b] Department of Chemistry and Physics, Faculty of Education, Alexandria University, Egypt.

[c] Theoretical Applied Chemistry Unit (TACU), Chemistry Department, Faculty of Science, Tanta University, Egypt.

[d] Department of Pharmaceutical Chemistry, Faculty of Pharmacy, Alexandria University, Alexandria, 21521, Egypt

Corresponding author mohamed.awad1@science.tanta.edu.eg

Table of content

1. Quantum chemical data for APCB

Table S1 Optimized structural parameters (bond length, bond angle and dihedral angle) of 2-amino-*N*-(phenylcarbamothioyl) benzamide.

Bonded atoms	**Bond Length (Å)**	**Bonded atoms**	**Bond angle (°)**	**Bonded atoms**	**Bond angle (°)**
C1-C2	1.409	C2,C1,C6	118.667	C18,N19,H21	112.818
C2-C3	1.381	C2,C1,C14	121.420	C18,N19,C22	132.497
C3-C4	1.401	C1,C2,C3	122.219	H21,N19,C22	114.673
C5-C6	1.413	C6,C1,C14	119.902	N19,C22,C23	115.257
C1-C6	1.426	C1,C6,C5	118.133	N19,C22,C24	125.443
C2-H7	1.084	C1,C6,N11	122.580	C23,C22,C24	119.298
C3-H8	1.082	C1,C14,O15	122.737	C22,C23,C25	120.602
C4-H9	1.084	C1,C14,N16	116.331	C22,C23,H26	119.475
C5-H10	1.085	C3,C2,H7	118.002	C22,C24,C27	119.414
C6-N11	1.366	C2,C3,C4	118.795	C22,C24,H32	119.951
N11-H12	1.009	C2,C3,H8	120.413	C25,C23,H26	119.922
N11-H13	1.006	C4,C3,H8	120.788	C23,C25,C28	120.208
C1-C14	1.479	C3,C4,C5	120.606	C23,C25,H29	119.455
C14-C15	1.240	C3,C4,H9	120.009	C27,C24,H32	120.633
C14-N16	1.382	C5,C4,H9	119.380	C24,C27,C28	121.321
N16-H17	1.008	C4,C5,C6	121.532	C24,C27,H30	118.716
N16-C18	1.411	C4,C5,H10	120.034	C28,C25,H29	120.335
C18-S20	1.673	C6,C5,H10	118.432	C25,C28,C27	119.155
C18-N19	1.346	C5,C6,N11	119.248	C25,C28,H31	120.369
N19-H21	1.023	C6,N11,H12	117.947	C28,C27,H30	119.962
N19-C22	1.412	C6,N11,H13	118.429	C27,C28,H31	120.474
C23-C25	1.387	N11,H12,O15	128.141	C18,N19,H21	112.818
C27-C28	1.391	C14,O15,H12	104.444	H21,N19,C22	114.673
C22-C24	1.399	C14,N16,H17	118.206	N19,C22,C23	115.257
C24-H32	1.078	C14,N16,C18	130.807	N19,C22,C24	125.443
C27-H30	1.084	H17,N16,C18	110.958	C23,C22,C24	119.298
C28-H31	1.083	N16,C18,N19	114.107		
C25-H29	1.084	C16,C18,S20	116.307		
C23-H26	1.085	N19,C18,S20	129.584		

Table S1 continued.

Atoms	Dihedral angle (°)
C4,C3,C2,C1	-0.178
C5,C4,C3,C2	1.063
C6,C5,C4,C3	-0.120
H7,C2,C1,C6	175.985
H8,C3,C2,C1	179.276
H9,C4,C3,C2	-179.638
H10,C5,C4,C3	179.383
N11,C6,C5,C4	-179.477
H12,N11,C6,C5	-165.909
H13,H11,C6,C5	-10.993
C14,C1,C2,C3	179.514
O15,C14,C1,C2	160.880
N16,C14,C1,C2	-19.767
H17,N16,C14,C1	6.506
C18,N16,C14,C1	175.607
N19,C18,N16,C14	0.938
S20,C18,N16,C14	-179.191
H21,N19,C18,N16	1.946
C22,N19,C18,N16	-179.355
C23,C22,N19,C18	-177.179
C24,C22,N19,C18	3.165
C25,C23,C22,N19	-179.858
H26,C23,C22,N19	0.173
C27,C24,C22,N19	179.795
C28,C27,C24,C22	-0.015
H29,C25,C23,C22	-179.933
H30,C27,C24,C22	179.955
H31,C28,C27,C24	179.932
H32,C24,C22,N19	-0.412

Table S2 Calculated and experimental vibrational frequencies for the title molecule

Mode	Experimental Frequency	Calculated Frequency		IR Intensity	Assignments and PED% contributions
	FT-IR	unscaled	scaled		
90		3699	3551	89.69	γNH (94)
89	3250	3620	3475	39.15	γNH (100)
88	3220	3557	3415	88.69	γNH (94)
87	3140	3354	3219	369.18	γNH (99)
86		3237	3107	9.71	γCH (98)
85		3200	3072	8.37	γCH (79) + γCH (11)
84		3191	3064	20.32	γCH (83)
83		3182	3052	19.49	γCH (15) + γCH (65) + γCH (16)
82		3179	3052	18.01	γCH (86)
81		3173	3046	0.42	γCH (75) + γCH (15)
80		3169	3042	0.72	γCH (81) + γCH (10)
79		3160	3033	8.85	γCH (20) + γCH (77)
78	3026	3159	3032	5.41	γCH (84)
77	1665	1693	1627	52.33	γCO (36) + βHNH (28)
76	1620	1658	1593	337.60	γCC (12) + γCC (10) + γCC (10) + γCC (20) + βHNH (10) + βHCC (11)
75		1645	1581	36.99	γCC (36) + βHCC (10)
74	1553	1637	1573	217.92	γCC (30) + βHNC (11)
73	1531	1621	1558	153.06	βHNH (37)
72		1604	1542	264.07	γCC (20) + βHNC (20)
71		1585	1523	277.46	γCC (23)
70	1490	1551	1490	625.99	γCN (13) + βHNC (54)
69	1337	1526	1466	114.64	βHCC (54) + βCCC (10)
68		1516	1457	11.58	βHCC (41) + βHCC (10)
67		1480	1422	19.35	γCC (12) + βHCC (17) + βHCC (19)
66		1478	1420	14.00	γCC (10) + βHCC (15) + βHCC (18)
65		1383	1329	499.52	γCN (35)
64		1371	1317	97.17	γCC (16) + γCC (19) + γCC (10) + γCC (12)
63		1358	1305	63.14	βHCC (75)
62		1350	1298	71.85	βHCC (42)
61		1342	1289	12.14	γCC (54)
60		1300	1249	39.68	γCC (37) + βHCC (10)
59		1269	1219	284.71	γCN (17)
58	1225	1239	1190	69.81	γCN (12) + γCN (16) + γCC (19)
57	1193	1205	1158	0.73	γCC (15) + βHCC (75)
56	1168	1195	1148	78.69	γCC (16) + βHNC (58)
55	1122	1186	1140	5.46	γCC (12) + βHCC (47)
54	1069	1183	1137	0.23	βHCC (82)
53		1155	1110	334.25	γCN (42) + βHNC (10)

52		1110	1067	0.64	γCC (24) + βHCC (42)
51		1085	1043	15.46	γCC (14) + γCC (23) + βHNC (20) + βHCC (12)
50		1072	1031	10.41	γCN (25) + βHCC (14)
49		1051	1010	9.36	γCC (41) + βHCC (23) + βCCC (20)
48	1031	1042	1001	16.25	γCC (12) + γCC (17) + γCC (17) + βHNC (24) + βCCC (12)
47	987	1013	974	0.31	γCC (15) + βCCC (49)
46	909	997	959	0.19	τHCCC (59) + τNCCC (13)
45		988	950	0.15	τHCCC (77) + τCCCC (11)
44		978	940	0.03	τHCCC (72)
43		965	927	3.24	γCN (11) + βCCC (26) + τHCCC (12)
42	885	952	915	0.41	τHCCC (58)
41		919	883	7.79	τHCCC (82)
40		882	847	13.16	βCCC (10) + βCNC (20)
39		857	824	7.83	τHCCN (63) + τHCCC (13)
38	843	849	816	14.64	τHNCC (25) + τHCCC (66)
37		827	794	3.61	βCCC (12) + βCCC (10) + βCCC (26)
36		821	789	41.63	τHNCC (53) + τHCCC (24)
35	801	789	758	18.16	τOCNC (42) + τNCCC (11)
34		769	739	34.05	τHCCC (60) + τCCCC (23)
33		759	729	44.08	τHCCC (49) + τHCCC (12) + τNCCC (10)
32	761	753	724	43.69	γCS (33)
31		707	679	1.83	τOCNC (32) + τNCCC (15)
30	689	702	675	30.59	τHCCC (16) + τHCCC (27) + τCCCC (43)
29		688	662	27.06	βHCC (43) + βCCC (10)
28	645	665	639	21.05	βNCS (61)
27		639	614	45.55	βHCC (82)
26		629	605	1.14	βCCC (51) + βCCC (24)
25		602	578	17.84	τSNNC (85)
24	569	582	559	20.60	τHNCC (64)
23	558	573	551	8.45	γCC (12) + βCCC (12) + βCCC (23)
22	528	540	519	24.78	τNCCC (17)
21		526	506	28.79	τNCCC (16)
20		517	497	9.95	τHCCC (11) + τNCCC (67)
19		454	437	3.16	βCCC (26) + τCCCC (10)
18		438	421	7.52	βCCC (38) + τCCCC (11)
17		419	403	3.62	γCC (14) + βCCC (45)
16		416	400	0.04	τHCCC (14) + τCCCC (81)
15		394	379	14.89	βCCN (46)
14		346	332	181.29	τHNCC (74)
13		318	306	2.96	βCCN (46)
12		271	260	1.46	τCNCN (45) + τCNCN (12)
11		249	240	6.24	βNCS (47) + τCCCC (10)
10		239	229	5.97	βNCS (13) + τCCCC (23) + τCCCC (13) + τCNCN (10)
9		199	191	6.93	βCCC (13) + βCCN (15) + βCCN (12)
8		171	164	0.97	βCCN (45) + τHCCC (14)

7		130	125	1.77	βCCN (21) + τHCCC (12) + τCCCC (11) + τCCCC (18)
6		115	110	2.02	τCCCC (14) + τCNCN (52)
5		87	83	0.94	τCNCN (59)
4		65	63	0.68	βCCN (70)
3		37	36	0.32	τCCCN (76)
2		24	23	0.56	τCCNC(76)
1		19	18	0.23	τCNCC (86)

Abbreviations: γ-stretching, β- bending, and τ-torsion modes.

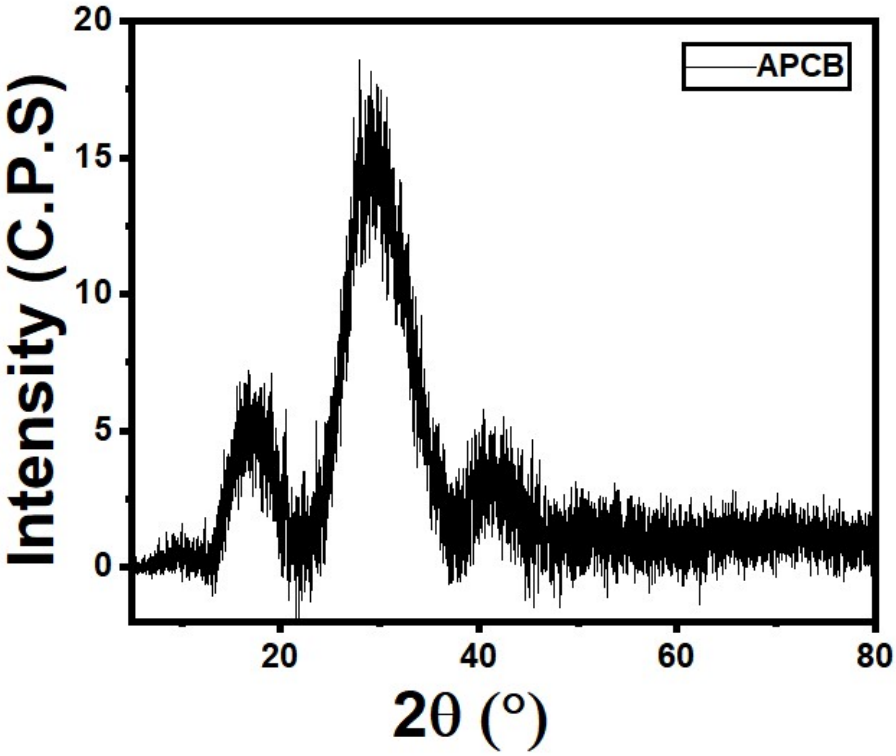

Fig.S1 PXRD data for investigated compound.

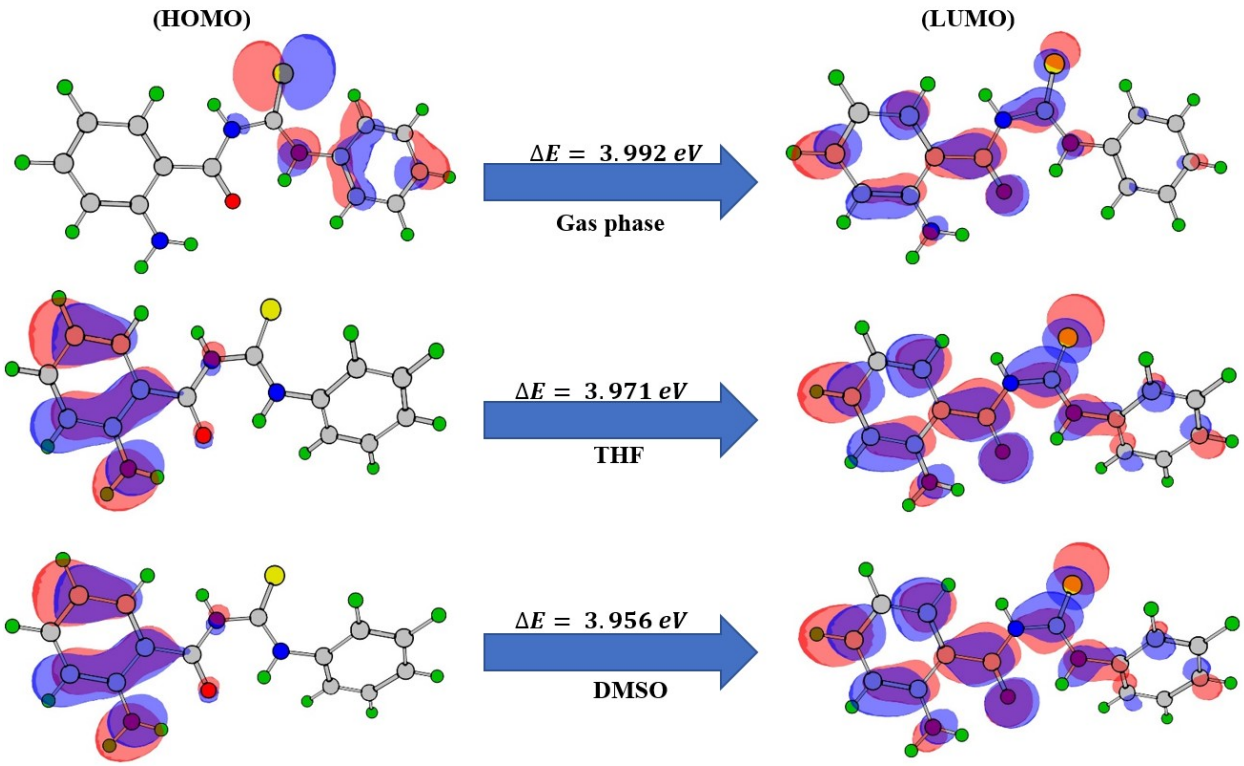

Fig. S2 Charge distribution density in HOMO and LUMO for APCB in gas phase, THF and DMSO solvents.

Table S3 Global reactivity descriptors for APCB in the gas phase, THF and DMSO solvents.

Molecular descriptor	**Gas phase**	**THF**	**DMSO**
E_{HOMO} (eV)	-6.163	-6.147	-6.138
E_{LUMO} (eV)	-2.171	-2.176	-2.182
ΔE (eV)	3.992	3.971	3.956
Ionization potential **(I = -E_{HOMO})** (eV)	6.163	6.147	6.138
Electron affinity **(A = -E_{LUMO})** (eV)	2.171	2.176	2.182
Chemical hardness $(\eta = (I - A)/2)$ (eV)	1.996	1.985	1.978
Chemical softness ($\sigma = {}^{1}/_{\eta}$) (eV)$^{-1}$	0.501	0.503	0.505
Absolute electronegativity $(\chi = (I + A)/2)$ (eV)	4.167	4.161	4.160
Chemical potential $(\mu = -(I + A)/2)$ (eV)	-4.167	-4.161	-4.160
Electrophilicity index $(\omega = {}^{\mu^2}/_{\eta})$ (eV)	8.699	8.722	8.749
Maximum charge transfer index($\Delta N_{max} = -{}^{\mu}/_{\eta}$)	2.087	2.096	2.103
μ_o (D)	4.775	6.403	6.827
$\langle\alpha\rangle$ (au)	236.689	301.647	318.118

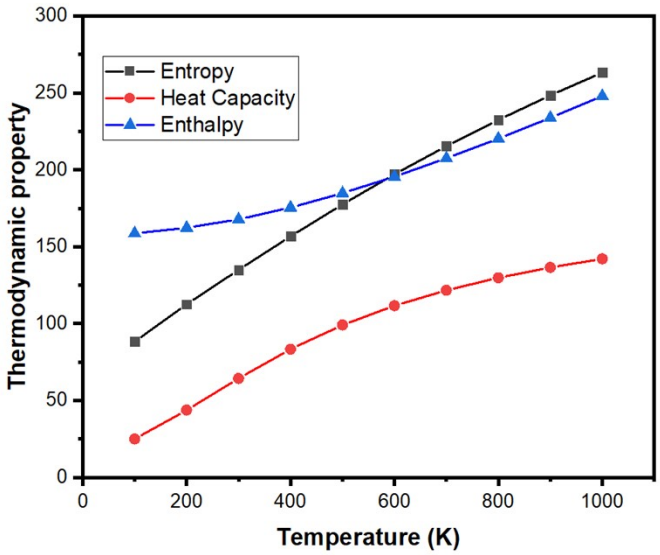

Fig. S3 Graphs depicting the temperature dependency of entropy, heat capacity, and enthalpy for APCB molecule.

Table S4 Calculated thermodynamic functions as a function of temperature.

T (K)	S (Cal.mol^{-1}.K^{-1})	C_V (Cal.mol^{-1}.K^{-1})	ΔH (kcal.mol^{-1})
100	88.340	24.956	158.723
200	112.558	43.705	162.326
300	134.991	64.360	167.883
400	156.756	83.357	175.543
500	177.550	99.099	184.898
600	197.144	111.658	195.667
700	215.437	121.686	207.560
800	232.495	129.824	220.350
900	248.418	136.547	233.887
1000	263.325	142.184	248.039

Table S5 The computed NLO parameters for APCB.

Descriptor	DFT/B3LYP/ 6-311++G(d,p)	Descriptor	DFT/B3LYP/ 6-311++G(d,p)
μ_x	-3.415	β_{xxx}	-55.603
μ_y	-3.309	β_{xyy}	-36.008
μ_Z	0.429	β_{xzz}	-4.939
μ_o (D)	4.775	β_{yyy}	-66.526
α_{xx}	344.642	β_{xxy}	-34.766
α_{xy}	-1.512	β_{yzz}	-0.801
α_{xz}	0.656	β_{zzz}	-1.296
α_{yy}	248.197	β_{xxz}	4.048
α_{yz}	2.433	β_{yyz}	2.409
α_{zz}	117.228	β_o (esu)	1.214×10^{-30}
α_o (esu)	3.507×10^{-23}		

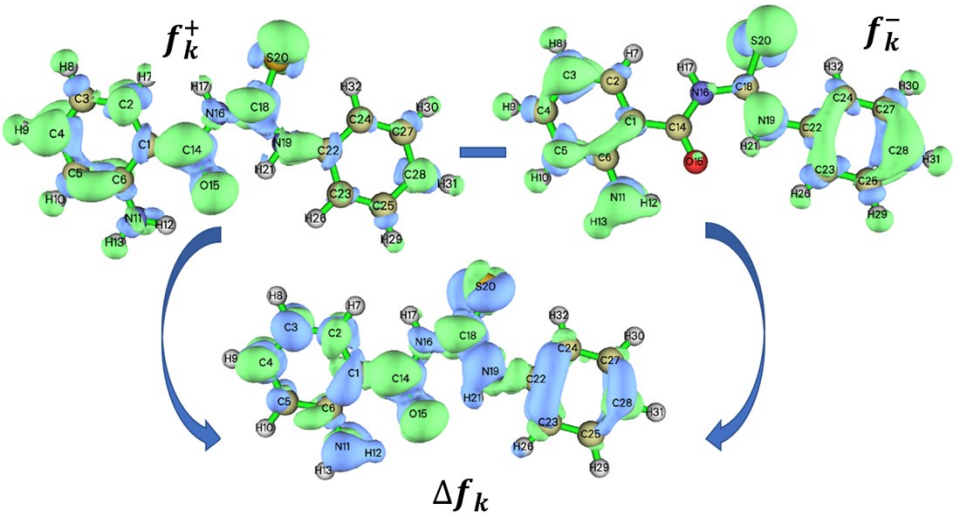

Fig. S4 Calculated f_k^+, f_k^-, and Δf_k for different atoms in APCB.

Table S6 Calculated values for the condensed Fukui functions.

Atom	f_k^+	f_k^-	Δf_k
C1	0.0059	-0.0183	0.0242
C2	-0.0470	-0.0192	-0.0277
C3	-0.0023	-0.0431	0.0407
C4	-0.0570	0.0031	-0.0611
C5	-0.0454	-0.0369	-0.0084
C6	-0.0143	-0.0009	-0.0134
N11	-0.0248	-0.0755	0.0506
C14	-0.0560	-0.0021	-0.0538
O15	-0.1011	-0.0219	-0.0791
N16	-0.0022	-0.0089	0.0066
C18	0.0144	0.0076	0.0068
N19	-0.0149	-0.0538	0.0388
S20	-0.2027	-0.1748	-0.0278
C22	-0.0156	-0.0674	0.0517
C23	-0.0389	-0.0370	-0.0019
C24	0.0224	0.0226	-0.0001
C25	0.0082	-0.0007	0.0090
C27	-0.0116	-0.0029	-0.0087
C28	-0.0286	-0.0406	0.0120

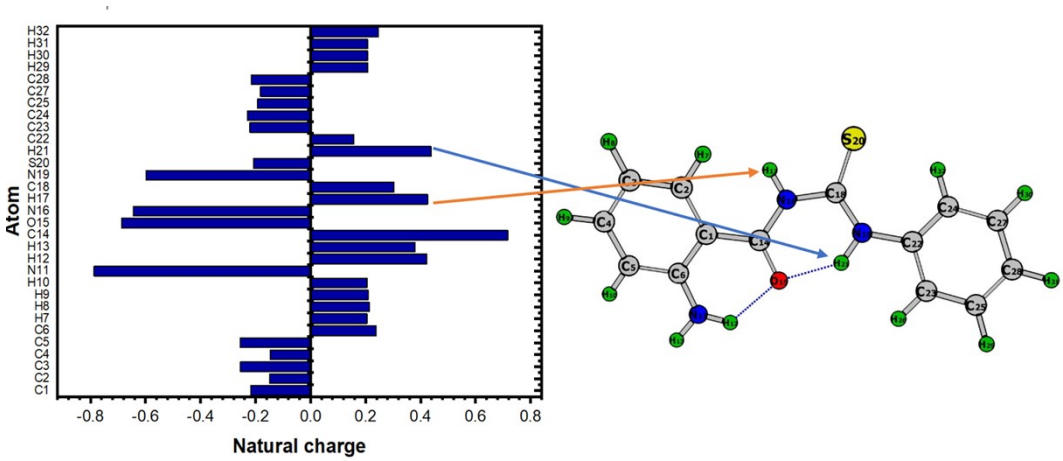

Fig. S5 The calculated natural charges for different atoms in APCB.

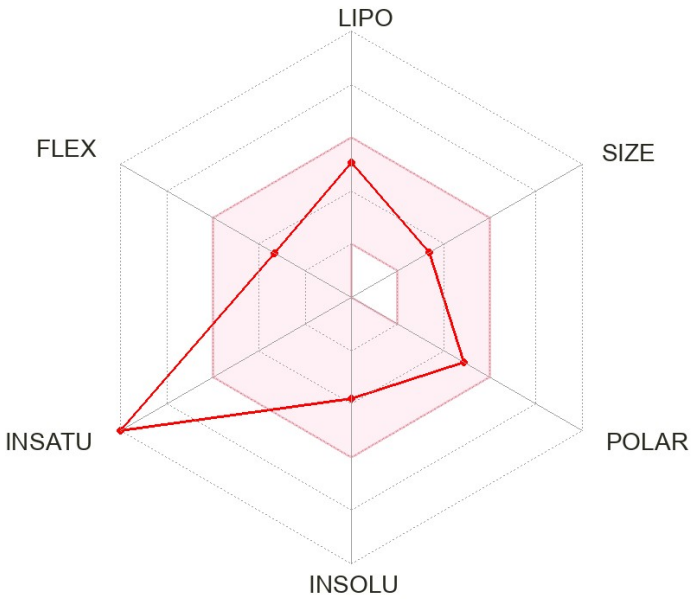

Fig. S6 The bioavailability of the investigated compound tested using the swissADME web application.

Table S7 Calculated drug-likeness properties for the APCB compound.

Calculated drug-likeness properties for title molecule	**Value**
Lipinski's violations	0
Hydrogen Bond Donor (HBD)	3
Hydrogen Bond Acceptor (HBA)	1
Topological polar surface area (TPSA) [$Å^2$]	99.24
Number of atoms	32
Number of rotatable bonds (NROTB)	5
Molecular weight (MW)	271.34
Consensus Log Po/w (clogP)	2.48
Bioavailability score	0.55

2. *The procedure of calculation for reduced density gradient*

1. Generate Gaussian file.
2. Copy and paste Multiwfn in the target file with the Gaussian file.
3. Open Multiwfn and press enter to select the file.
4. Select 20 representing Visual study of weak interactions.
5. Select 1 NCI analysis(also known as RDG analysis)
6. Select 3 High-quality grids.
7. Select -7 to show the isosurface of RDG.
8. After selecting a suitable isovalue, press -1 to draw a scatter graph.
9. The RDG will be shown in a non-colored manner.
10. To illustrate NCI within the molecule, copy and paste the VMD file into the desired file.
11. From the original Multiwfn software file, copy RDGfill.VMD from examples to the desired file.
12. Open VMD and write soure RDGfill.VMD.
13. The interaction is observed in a new window.

3.1. MTT assay against MCF-7 cells

3.1.1. Mammalian cell lines: MCF-7 cells (human breast cancer cell line), were obtained from the American Type Culture Collection (ATCC, Rockville, MD).

3.1.2. Chemicals Used: Dimethyl sulfoxide (DMSO), MTT and trypan blue dye were purchased from Sigma (St. Louis, Mo., USA).

Fetal Bovine serum, RPMI-1640, HEPES buffer solution, L-glutamine, gentamycin and 0.25% Trypsin-EDTA were purchased from Lonza (Belgium).

3.1.3. <u>Cell line Propagation:</u>

The cells were grown on RPMI-1640 medium supplemented with 10% inactivated fetal calf serum and 50µg/ml gentamycin. The cells were maintained at 37ºC in a humidified atmosphere with 5% CO2 and were subcultured two to three times a week.

3.1.4. Cytotoxicity evaluation using viability assay

For antitumor assays, the tumor cell lines were suspended in medium at concentration $5x10^4$ cell/well in Corning® 96-well tissue culture plates, then incubated for 24 hr. The tested

compounds were then added into 96-well plates (three replicates) to achieve twelve concentrations for each compound. Six vehicle controls with media or 0.5 % DMSO were run for each 96 well plate as a control. After incubating for 24 h, the numbers of viable cells were determined by the MTT test. Briefly, the media was removed from the 96 well plate and replaced with 100 µl of fresh culture RPMI 1640 medium without phenol red then 10 µl of the 12 mM MTT stock solution (5 mg of MTT in 1 mL of PBS) to each well including the untreated controls. The 96 well plates were then incubated at 37°C and 5% CO_2 for 4 hours. An 85 µl aliquot of the media was removed from the wells, and 50 µl of DMSO was added to each well and mixed thoroughly with the pipette and incubated at 37°C for 10 min. Then, the optical density was measured at 590 nm with the microplate reader (SunRise, TECAN, Inc, USA) to determine the number of viable cells and the percentage of viability was calculated as [(ODt/ODc)]x100% where ODt is the mean optical density of wells treated with the tested sample and ODc is the mean optical density of untreated cells. The relation between surviving cells and drug concentration is plotted to get the survival curve of each tumor cell line after treatment with the specified compound. The 50% inhibitory concentration (IC_{50}), the concentration required to cause toxic effects in 50% of intact cells, was estimated from graphic plots of the dose response curve for each conc. using Graphpad Prism software (San Diego, CA. USA).

3.2. MTT assay against MRC-5 cells.

3.2.1. Mammalian cell lines: MRC-5

(Normal human Lung fibroblast cells), were obtained from the American Type Culture Collection (ATCC, Rockville, MD).

3.2.2. Chemicals Used

Dimethyl sulfoxide (DMSO), MTT and trypan blue dye were purchased from Sigma (St. Louis, Mo., USA). Fetal Bovine serum, DMEM, HEPES buffer solution, L-glutamine, gentamycin and 0.25% Trypsin-EDTA were purchased from Lonza (Belgium).

3.2.3. <u>Cell line Propagation</u>

The cells were propagated in Dulbecco's modified Eagle's medium (DMEM) supplemented with 10% heat-inactivated fetal bovine serum, 1% L-glutamine, HEPES buffer and 50µg/ml gentamycin. All cells were maintained at 37ºC in a humidified atmosphere with 5% CO_2 and were subcultured two times a week.

3.2.4. Cytotoxicity evaluation using viability assay

For cytotoxicity assay, the cells were seeded in 96-well plate at a cell concentration of 1×10^4 cells per well in 100µl of growth medium. Fresh medium containing different concentrations of the test sample was added after 24 h of seeding. Serial two-fold dilutions of the tested chemical compound were added to confluent cell monolayers dispensed into 96-well, flat-bottomed microtiter plates (Falcon, NJ, USA) using a multichannel pipette. The microtiter plates were incubated at 37ºC in a humidified incubator with 5% CO_2 for a period of 24 h. Three wells were used for each concentration of the test sample. Control cells were incubated without test sample and with or without DMSO. The little percentage of DMSO present in the wells (maximal 0.1%) was found not to affect the experiment. After incubation of the cells viable cells yield was determined by a colorimetric method.

After incubating for 24 h, the numbers of viable cells were determined by the MTT test. Briefly, the media was removed from the 96 well plate and replaced with 100 µl of fresh culture RPMI 1640 medium without phenol red then 10 µl of the 12 mM MTT stock solution (5 mg of MTT in 1 mL of PBS) to each well including the untreated controls. The 96 well plates were then incubated at 37°C and 5% CO_2 for 4 hours. An 85 µl aliquot of the media was removed from the wells, and 50 µl of DMSO was added to each well and mixed thoroughly with the pipette and incubated at 37°C for 10 min. Then, the optical density was measured at 590 nm with the microplate reader (SunRise, TECAN, Inc, USA) to determine the number of viable cells and the percentage of viability was calculated as [(ODt/ODc)]x100% where ODt is the mean optical density of wells treated with the tested sample and ODc is the mean optical density of untreated cells.

The relation between surviving cells and drug concentration is plotted to get the survival curve of each tumor cell line after treatment with the specified compound. The Cytotoxic concentration (CC_{50}), the concentration required to cause toxic effects in 50% of intact cells, was estimated from

graphic plots of the dose response curve for each conc. using Graphpad Prism software (San Diego, CA. USA).

3.3. VEGFR-2 kinase inhibitory activity assay

The most active compound was evaluated for in vitro VEGFR-2 kinase inhibitory activity by VEGFR2 (KDR) Kinase Assay Kit-BPS Bioscience Corporation catalog # 40325, using Kinase-Glo® MAX as a detection reagent following the manufacturer's instructions as following:

- Thaw 5x Kinase Buffer 1, ATP and PTK substrate Poly (Glu:Tyr 4:1) (10 mg/ml).

- Prepare the master mixture (25 µl per well): N wells x (6 µl 5x Kinase Buffer 1 + 1 µl ATP (500 µM) + 1 µl PTK substrate Poly (Glu:Tyr 4:1) (10 mg/ml)+ 17 µl water). Add 25 µl to every well.

- Add 5 µl of Inhibitor solution of each well labeled as "Test Inhibitor". For the "Positive Control" and "Blank", add 5 µl of the same solution without inhibitor (Inhibitor buffer).

- Prepare 3 ml of 1x Kinase Buffer 1 by mixing 600 µl of 5x Kinase Buffer 1 with 2400 µl water. 3 ml of 1x Kinase Buffer 1 is sufficient for 100 reactions.

- To the wells designated as "Blank", add 20 µl of 1x Kinase Buffer 1.

- Thaw VEGFR2 enzyme on ice. Upon first thaw, briefly spin tube containing enzyme to recover full content of the tube. Calculate the amount of VEGFR2 required for the assay and dilute enzyme to 1 ng/µl with 1x Kinase Buffer 1.

- Initiate reaction by adding 20 µl of diluted VEGFR2 enzyme to the wells designated "Positive Control" and "Test Inhibitor Control". Incubate at 30°C for 45 minutes.

- Thaw Kinase-Glo Max reagent.

- After the 45 minutes, add 50 µl of Kinase-Glo Max reagent to each well. Cover plate with aluminum foil and incubate the plate at room temperature for 15 minutes.

- Measure luminescence using the microplate reader.

- Inhibitory activity was expressed as IC_{50} values (the concentration at which 50 % of the enzyme activity inhibited), which were calculated from dose-response curves obtained using twelve tested concentrations of the inhibitor and carried out in duplicate as shown below:

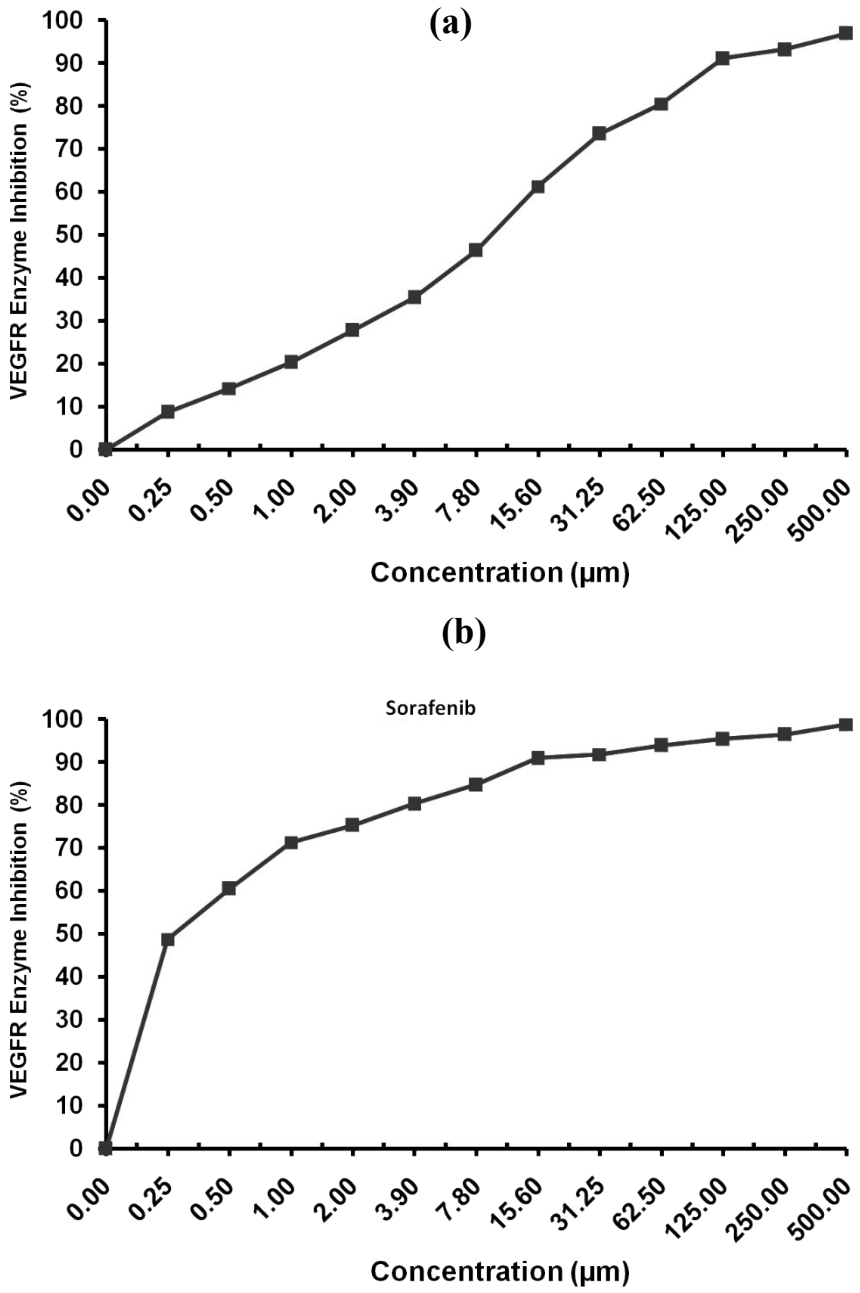

Fig. S7 Relation between VEGFR-2 enzyme inhibition as a function of concentration for (a) head molecule. (b) sorafenib.

Table S8 Inhibition of VEGFR-2 Enzyme in the presence of various concentrations of APCB.

Sample conc. (µm)	% of VEGFR Enzyme Activity	VEGFR Enzyme Inhibition (%)	S.D. (±)
500	3.11	96.89	0.27
250	6.86	93.14	0.38
125	8.92	91.08	0.74
62.5	19.53	80.47	0.91
31.25	26.48	73.52	1.46
15.6	38.72	61.28	0.94
7.8	53.63	46.37	1.05
3.9	64.59	35.41	0.63
2	72.18	27.82	0.44
1	79.61	20.39	0.23
0.5	85.75	14.25	0.17
0.25	91.27	8.73	0.09
0	100	0	

Table S9 Inhibition of VEGFR-2 Enzyme in the presence of various concentrations of sorafenib.

Sample conc. (µg/ml)	% of VEGFR Enzyme Activity	VEGFR Enzyme Inhibition (%)	S.D. (±)
500	1.24	98.76	0.32
250	3.58	96.42	0.46
125	4.63	95.37	0.21
62.5	6.11	93.89	0.53
31.25	8.24	91.76	0.28
15.6	9.07	90.93	0.11
7.8	15.28	84.72	0.06
3.9	19.71	80.29	0.37
2	24.66	75.34	0.28
1	28.71	71.29	0.65
0.5	39.47	60.53	1.29
0.25	51.29	48.71	0.83
0	100	0	

Table S10 Comparison of IC_{50} of the investigated compound to other recently published thiourea derivative and reference compound.

Compound	**IC_{50}**
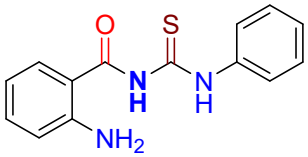	(investigated compound) 35.78 µM
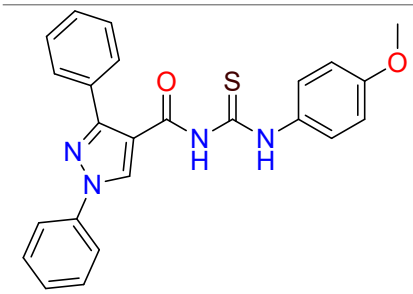	>5000 nM
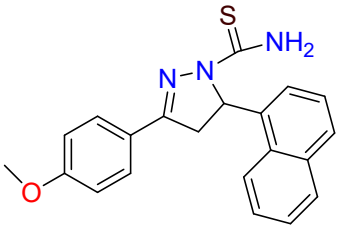	4.1 µM
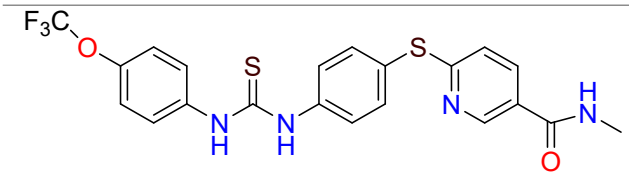	>10000 nM
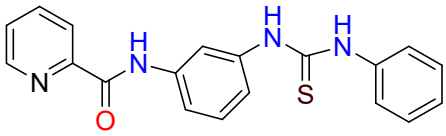	100.00 nM
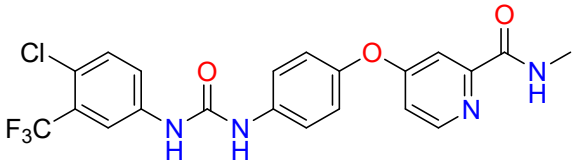	4.92 nM